

Excited State Dynamics of Ru(bpy)₃²⁺ on Porous Vycor Glass. Intervention of a Ligand Localized Triplet State

Jianwei Fan,[†] Steven Tysoe,[‡] Thomas C. Streckas,[§] Harry D. Gafney,^{*§} Nick Serpone,[⊥] and Darren Lawless[⊥]

Contribution from the Department of Chemistry and Biochemistry, Manhattan College, Riverdale, New York 10471, Department of Chemistry, St. Mary's College, St. Mary's City, Maryland 20686, Department of Chemistry and Biochemistry, City University of New York, Queens College, Flushing, New York 11367, and Canadian Centre for Picosecond Laser Flash Photolysis, Department of Chemistry, Concordia University, Montreal, Quebec, Canada H3G 1M8

Received November 29, 1993*

Abstract: Absorption and emission spectra of Ru(bpy)₃²⁺ cation exchanged onto porous Vycor glass (PVG) closely resemble the corresponding aqueous solution spectra. However, complementary measurements of emission lifetime and quantum yield, Φ_{em} , reveal that, unlike fluid solution behavior where the ratio is temperature independent, the Φ_{em}/τ ratio declines by 42% in the 5 to 90 °C range. The temperature dependence is due to the intersystem crossing efficiency, η_{isc} , and a model consistent with both emission quantum yield and lifetime data indicates that the temperature dependence arises from the thermal population of a level that lies $1117 \pm 70 \text{ cm}^{-1}$ above the ¹MLCT state. This level is assigned to a ligand localized triplet state, ³LL, and population of this state leads to nonradiative decay competitive with intersystem crossing to the emissive manifold. As a result, the apparent intersystem crossing efficiency declines with increasing temperature. Although it is generally accepted that the intersystem crossing efficiency of Ru(II) diimines is independent of temperature, comparisons with currently available data show that η_{isc} can either increase or decrease with temperature when the complex possesses an asymmetric coordination environment. The asymmetry arises either from different ligands coordinated to Ru(II) or with Ru(bpy)₃²⁺ cation exchanged onto PVG, a differentiation of the initially equivalent ligands by the anionic surface of the glass. Under these conditions, intersystem crossing efficiency either increases or decreases with temperature depending on the relative energies of the ¹MLCT and ³LL states.

Introduction

While the energy crisis focused attention on their photoredox properties,¹ more recent studies have taken advantage of the luminescence of Ru(II) diimines to probe the structure and environment of biological and inorganic supports.^{2–11} Inferences regarding microstructure and microenvironment are usually drawn from changes in absorption and emission energy, emission lifetime and quantum yield, and polarization ratio of the complex in a specific medium relative to that found in fluid solution. Implicit in many of these comparisons, however, is the assumption that the complex's photophysical processes prior to emission remain equivalent to those in the reference medium.

Information regarding the states involved in the emission process, their decay dynamics, and particularly the events preceding emission derives from the temperature dependence of emission quantum yield, Φ_{em} , and lifetime, τ . Low-temperature data reveal an emissive manifold in Ru(bpy)₃²⁺ composed of three levels that differ in energy by $\leq 80 \text{ cm}^{-1}$, while fluid solution data reveal temperature-independent radiative, k_r , and nonradiative, k_{nr} , pathways that directly couple the emissive and ground states.^{12–16} Temperature-dependent nonradiative pathways have also been identified that couple the emissive state to the ground state via the population of a higher energy manifold. Van Houton and Watts assigned the higher energy state in Ru(bpy)₃²⁺ to a d–d manifold that lies ca. 3600 cm^{-1} above the emissive state.¹⁶ In mixed-ligand Ru(II) complexes, however, the energy of the proposed dd manifold does not parallel ligand field strength, and in contrast to Ru(bpy)₃²⁺ which undergoes photolabilization at higher temperatures,¹⁶ many Ru(II) and Os(II) polypyridal complexes exhibit little or no photolabilization of a coordinated ligand.^{19–22} Also, incorporating Ru(bpy)₃²⁺ into a dry cellulose acetate film has relatively little effect on the complex's absorption

[†] Manhattan College.

[‡] St. Mary's College.

[§] Queens College.

[⊥] Concordia University.

* Abstract published in *Advance ACS Abstracts*, May 15, 1994.

(1) (a) Kalyanasundram, K. *Coord. Chem. Rev.* **1982**, *46*, 159. (b) Juris, A.; Balzani, V.; Barigelletti, F.; Campagna, S.; Belser, P.; von Zelewsky, A. *Coord. Chem. Rev.* **1988**, *84*, 85.

(2) Pyle, A. M.; Barton, J. K. In *Progress in Inorganic Chemistry: Bioinorganic Chemistry*; Lippard, S. J., Ed.; John Wiley & Sons: New York, 1990; Vol. 38, pp 413–475.

(3) Eriksson, M.; Lejon, M.; Hirot, C.; Norden, B.; Graslund, A. *J. Am. Chem. Soc.* **1992**, *114*, 4933.

(4) Satyanarayana, S.; Dabrowiak, J. C.; Chaires, J. B. *Biochemistry* **1992**, *31*, 9319.

(5) Tossi, A. B.; Kelly, J. M. *Photochem. Photobiol.* **1989**, *5*, 545.

(6) Baker, A. D.; Morgan, R. J.; Streckas, T. C. *Inorg. Chem.* **1991**, *30*, 2687.

(7) Haworth, I. S.; Elcock, A. H.; Freeman, J.; Rodger, A.; Richards, W. G. *J. Biomol. Struct. Dyn.* **1991**, *9*, 23.

(8) Thomas, J. K. *Chem. Rev.* **1980**, *80*, 283; *J. Phys. Chem.* **1987**, *91*, 267.

(9) Krenke, D.; Abdo, S.; Van Damme, H.; Cruz, M.; Fripat, J. J. *J. Phys. Chem.* **1980**, *84*, 2447; **1981**, *85*, 797.

(10) Shi, W.; Wolfgang, S.; Streckas, T. C.; Gafney, H. D. *J. Phys. Chem.* **1985**, *89*, 974.

(11) Gafney, H. D. *Coord. Chem. Rev.* **1990**, *104*, 113.

(12) Demas, J. N.; Crosby, G. A. *J. Am. Chem. Soc.* **1971**, *93*, 2841.

(13) Harrigan, R. W.; Crosby, G. A. *J. Chem. Phys.* **1973**, *59*, 3468.

(14) Harrigan, R. W.; Hager, G. D.; Crosby, G. A. *Chem. Phys. Lett.* **1973**, *21*, 487.

(15) Harrigan, R. W.; Crosby, G. A. *J. Chem. Phys.* **1973**, *59*, 3468.

(16) Van Houton, J.; Watts, R. J. *J. Am. Chem. Soc.* **1976**, *98*, 4853.

(17) A Lumpkin, R. S.; Meyer, T. J. *J. Phys. Chem.* **1986**, *90*, 5307. (b) Danielson, E.; Lumpkin, R. S.; Meyer, T. J. *J. Phys. Chem.* **1987**, *91*, 1305.

(c) Ferguson, J.; Krausz, E. F.; Maeder, M. J. *J. Phys. Chem.* **1985**, *89*, 1582. (d) Ferguson, J.; Krausz, E. *Chem. Phys. Lett.* **1986**, *127*, 551. (e) Kitamura, N.; Kim, H.; Kawanishi, Y.; Obata, R.; Tazuke, S. *J. Phys. Chem.* **1986**, *90*, 1488. (f) Ferguson, J.; Krausz, E. *Chem. Phys. Lett.* **1988**, *143*, 77.

(18) Allsopp, S. R.; Cox, A.; Kemp, T. J.; Reed, W. J. *J. Chem. Soc., Faraday Trans. 1* **1978**, *74*, 1275; **1979**, *75*, 353.

(19) Barigelletti, F.; Juris, A.; Balzani, V.; Belser, P.; von Zelewsky, A. *Inorg. Chem.* **1983**, *22*, 3335.

(20) Allen, G. H.; White, R. P.; Rillema, D. P. *J. Am. Chem. Soc.* **1984**, *106*, 2613.

spectrum, but it reduces the activation barrier to $810 \pm 120 \text{ cm}^{-1}$.¹⁸ In these cases, lifetime vs temperature data yield activation barriers of 300–800 cm^{-1} that are assigned to the population of a lower lying MLCT state.^{19–22} A low-lying MLCT state, designated $2A_2'$, has been identified ca. 800 cm^{-1} above the emissive E' state in $[\text{Ru}(\text{bpy})_3](\text{PF}_6)_2$ single crystals,²³ and population of this state in the cellulose acetate matrix, as opposed to a dd state in aqueous solution, is attributed to “matrix effects”, *i.e.*, the rigidity of the surrounding matrix curtails the molecular vibrations required to access the dd manifold.²²

In contrast to the detail regarding the emissive states and their relaxation dynamics, little attention has been paid to the events preceding emission. In fact, it is generally assumed that the intersystem crossing, η_{isc} , of Ru(II) and Os(II) diimines is unity and independent of temperature, molecular structure, and experimental conditions. In spite of the generality of its application, the assumption is based on little experimental data. In low-temperature matrices, Φ_{em} has been shown to be independent of excitation wavelength, and it was suggested that η_{isc} is unity.¹² In aqueous solution, Φ_{em} is also independent of excitation wavelength, and in the 273–373 K range, the ratio Φ_{em}/τ , which is proportional to η_{isc} , is independent of temperature.¹⁶ Intersystem crossing, however, is a radiationless process, and while it may be facilitated by the spin–orbit coupling of these metals, it is by no means clear, as is currently assumed, that it is always unity and independent of molecular structure, temperature, and the medium to which the energy is dissipated. Particularly as their use as luminescent probes of microstructure and microenvironment increases, the assumption that the events preceding emission are equivalent to those in the reference medium must be established.

Our interest in the intersystem crossing efficiency of Ru(II) diimines stems from studies of the photoredox behavior of $\text{Ru}(\text{bpy})_3^{2+}$ in porous Vycor glass (PVG).^{11,24,25} The glass is being examined as a means of organizing a reaction system, but an equally important aspect is using the complex as a spectroscopic probe of glass's microstructure and microenvironment.¹⁰ The similarity of the spectroscopic properties of the complex adsorbed onto the glass with those in aqueous solution suggests a direct comparison.¹⁰ However, a number of observations, although individually inconclusive, collectively suggested that adsorption changes not only the dynamics of emission decay but also the decay dynamics prior to emission.¹¹ Specifically, the data raised the question of whether η_{isc} was an invariant parameter as is currently assumed. Consequently, the temperature dependence of Φ_{em} and τ for $\text{Ru}(\text{bpy})_3^{2+}$ cation exchanged onto porous Vycor glass, designated $\text{Ru}(\text{bpy})_3^{2+}(\text{ads})$, has been measured and compared to that in aqueous solution. The temperature dependence of the emission lifetime is in excellent agreement with previous results, and along with the photochemistry of the adsorbed complex, this suggests that the rigidity of the glass promotes the population of a nonemissive charge transfer state rather than a dd state. The Φ_{em}/τ ratio is independent of temperature for aqueous solution but declines by 42% in the 273–373 K range for $\text{Ru}(\text{bpy})_3^{2+}(\text{ads})$. The decline is attributed to η_{isc} , and a model consistent with both lifetime and emission quantum yield data indicates that the temperature dependence arises from the thermal population of an energy level that lies $1117 \pm 70 \text{ cm}^{-1}$ above the $^1\text{MLCT}$ state. This higher energy level is assigned to a ligand localized triplet state, ^3LL , and population of this state leads to nonradiative decay at the expense of intersystem crossing to the emissive manifold. Correlations with other data suggest that,

when the complex possesses an asymmetric coordination environment, intersystem crossing efficiencies of Ru(II) diimines either increase or decrease with temperature. The asymmetry arises either from different ligands coordinated to Ru(II) or, in the case of $\text{Ru}(\text{bpy})_3^{2+}(\text{ads})$, a differentiation of the equivalent bipyridine ligands due to adsorption onto the anionic surface of the glass. Under these conditions, where the energies of the individual ligand states differ, the intersystem crossing efficiency either increases or decreases with increasing temperature depending on the energy of the ^3LL state relative to that of the spectroscopically accessible $^1\text{MLCT}$ state.

Experimental Section

Materials. $[\text{Ru}(\text{bpy})_3]\text{Cl}_2$ was prepared by the method of Palmer and Piper²⁶ and twice recrystallized from distilled water. Absorption, emission, and resonance Raman spectra of aqueous solutions of the complex, prepared with distilled, deionized water, were in excellent agreement with published spectra.^{10,24} Code 7930 porous Vycor glass (Corning Inc.), either in the form of 25 mm \times 9 mm \times 1.1 mm glass plates or 250 to 1000 μm diameter particles, were extracted and calcined according to previously described procedures.^{10,24,27} All glass samples were calcined for at least 72 h prior to use and stored at 650 $^\circ\text{C}$ until needed.

Sample Preparation. Calcined samples were cooled to room temperature under vacuum and impregnated by previously described cation exchange procedures.^{10,24} The moles of $\text{Ru}(\text{bpy})_3^{2+}$ adsorbed onto the glass were measured spectroscopically, and $\geq 99.97\%$ of the water incorporated during impregnation was removed under vacuum at room temperature. All measurements were carried out with dry samples containing from 10^{-7} to 1.8×10^{-6} mol of $\text{Ru}(\text{bpy})_3^{2+}(\text{ads})/\text{g}$ of PVG.

Impregnated glass particles were placed in 2 mm diameter quartz tubes equipped with a vacuum stopcock and maintained under a dynamic vacuum ($\leq 5 \times 10^{-5}$ Torr) at room temperature for at least 12 h prior to any measurement. The degassed samples were cooled to 77 K in a quartz liquid N_2 dewar, and the emission spectra were recorded in a conventional manner.²⁷ Measurements in the 273–368 $^\circ\text{C}$ range were carried out with impregnated 25 mm \times 9 mm \times 1.1 mm plates. Quantitating the emission intensity from these samples, however, rested on minimizing two sources of error. The first is referred to as a positioning error and arises from the uncertainty introduced by removing and replacing the same or different glass samples in the emission spectrometer. To reduce this error, it was necessary to mount the impregnated plates in a 40 mm \times 10 mm \times 2 mm quartz cell and mount the cell in a thermostated cell holder machined to the dimensions of the quartz cell. Tests with the same sample and with different samples containing the same loadings showed that the tight fit of the sample in the cell and the cell in the sample holder reduced the repositioning error to $\leq 2\%$.

The second potential source of error concerned the removal of adsorbed O_2 . Since O_2 strongly adsorbs onto the glass and quenches the excited complex and the amount adsorbed declines with increasing temperature,²⁸ its presence introduces a systematic error in the observed temperature dependence. All samples, whether impregnated plates or glass particles, were degassed under a dynamic vacuum ($\leq 5 \times 10^{-5}$ Torr) at room temperature for at least 12 h prior to measurement. Since the amount of O_2 adsorbed decreases with increasing temperature, the reliability of the degassing procedure was tested by first degassing impregnated samples at room temperature, measuring their emission intensities and lifetimes, and then repeating the procedure with the samples maintained at 80 $^\circ\text{C}$ during evacuation. Absorption spectra recorded before and after evacuation at 80 $^\circ\text{C}$ established that $\text{Ru}(\text{bpy})_3^{2+}(\text{ads})$ was unaffected by the higher temperature. Emission intensities and lifetimes after degassing at 80 $^\circ\text{C}$ were within experimental error of those obtained after degassing at room temperature and confirmed the reliability of the degassing procedure.

Photolysis Procedures. $\text{Ru}(\text{bpy})_3^{2+}$ impregnated glass samples were mounted in 1 cm \times 1 cm quartz cells and evacuated to a pressure of $\leq 10^{-4}$ Torr. The evacuated cell was then placed in a cell holder thermostated with a Haake Model FK2 constant temperature bath and mounted in a Rayonet Photochemical Reactor (Southern New England Ultraviolet Corp.). The sample was irradiated with 350-nm light, and the excitation intensity was determined by ferrioxalate actinometry.²⁹ The reaction

(21) Wacholtz, W. M.; Auerbach, R. A.; Schmehl, R. H. *Inorg. Chem.* **1986**, *25*, 227.

(22) Lumpkin, R. S.; Kober, E. M.; Worl, L. A.; Murtaza, Z.; Meyer, T. *J. J. Phys. Chem.* **1990**, *94*, 239.

(23) Yersin, H.; Gallhuber, E. *J. Am. Chem. Soc.* **1984**, *106*, 6582.

(24) Kennelly, T.; Gafney, H. D.; Braun, M. *J. Am. Chem. Soc.* **1985**, *107*, 4431.

(25) Shi, W.; Gafney, H. D. *J. Am. Chem. Soc.* **1987**, *109*, 1582.

(26) Palmer, R. A.; Piper, T. S. *Inorg. Chem.* **1966**, *5*, 864.

(27) Fan, J.; Shi, W.; Tysoe, S.; Streckas, T. C.; Gafney, H. D. *J. Phys. Chem.* **1989**, *93*, 373.

(28) Wolfgang, S.; Gafney, H. D. *J. Phys. Chem.* **1983**, *87*, 5395.

was monitored spectrally and the amount of Ru(bpy)₃²⁺(ads) reacted was calculated from the change in absorbance at 452 nm according to the procedure of Wong and Allen.³⁰

Physical Measurements. UV-visible and resonance Raman spectra were recorded on an Aviv Model 14DS spectrophotometer and a previously described resonance Raman spectrometer.¹⁰ Emission spectra were recorded on a Perkin-Elmer Hitachi MPF-2A emission spectrophotometer equipped with a red-sensitive Hamamatsu R818 photomultiplier and a thermostated cell holder connected to the Haake constant temperature bath. The sample holder rigidly held the sample at an angle of 60° relative to the excitation axis. All samples were excited with light corresponding to the maximum of the MLCT absorption, and their emission spectra were recorded at 90° to the excitation axis. A filter that transmitted wavelengths ≥480 nm was placed between the sample and the emission monochromator to eliminate the scattered excitation light.

Emission quantum yields at the different temperatures were calculated from the equation³¹

$$\Phi_x = \Phi_r(I_x/I_r)(n_x^2/n_r^2) \quad (1)$$

where x and r refer to the adsorbed complex and a reference. All data were referenced to a degassed, aqueous solution of Ru(bpy)₃²⁺ contained in an identical 2 mm pathlength quartz cell. The concentration of the reference solution was adjusted to have the same optical density as the glass sample at the excitation wavelength, and all reference solutions were degassed by at least 3 freeze-pump-thaw cycles. Emission intensities from the glass samples, I_x , and the corresponding aqueous solutions, I_r , were measured under equivalent conditions and then compared to that obtained from a degassed, aqueous solution of Ru(bpy)₃²⁺ at 298 K where $\Phi_{em} = 0.042 \pm 0.002$.

Within experimental error, the refractive indices of water, $n_r = 1.33$, and consolidated glass are independent of temperature in the 5–95 °C range. It was not clear, however, whether this was also true for the porous glass used in these experiments. Consequently, the temperature dependence of its refractive index, n_x , was determined with a Michelson interferometer.³² The change in refractive index, Δn_x , was computed from the relation $2d\Delta n_x = k\lambda/2$, where k is the number of fringe lines displaced, λ is the wavelength, 633 nm, and d is the sample thickness, 1.1 ± 0.01 mm. Using a He-Ne laser, tests with the empty quartz cell showed no change in the fringe pattern in the 5–95 °C range. A calcined PVG sample was then placed in the cell, evacuated to a pressure of $\leq 5 \times 10^{-6}$ Torr, and the fringe pattern monitored as the temperature was raised from 5 to 95 °C. The lack of change indicated that the refractive index of the glass changed by $\leq 0.01\%$ over the entire temperature range. Consequently, n_x was taken to be 1.51, and independent of temperature.

Emission lifetimes were determined by previously described procedures.²⁷ The aqueous reference solutions and glass samples were degassed as described, mounted in thermostated cell holders, and excited with the 355-nm harmonic (7 nsec fwhm, 0.01 mJ/pulse) from a Quanta Ray Model DCR-2A Nd:YAG laser. Decays of the aqueous solutions of Ru(bpy)₃²⁺ were monitored at 90° to the excitation axis, while that of the adsorbed complex was monitored either through the edge of the sample, in which case the sample was mounted at 90° to the excitation axis, or from the front surface of the sample, in which case the sample was mounted at 60° to the excitation axis. All decays were monitored at their respective maxima, and consistent with previous results, the decays of the adsorbed complex were independent of the excitation-analysis geometry.^{27,33}

Picosecond experiments were performed to probe the multicomponent decays found in the impregnated glass samples. Impregnated glass samples at room temperature were excited with the 355-nm harmonic (ca. 30 ps fwhm, 1–2 mJ/pulse) from a passively mode locked Nd:YAG laser. Luminescence decays and transient absorption spectra were recorded as previously described.³⁴ Identical experiments with unimpregnated samples of the calcined glass showed that a fast component, $\tau \leq 50$ ns, that proceeds from the slower exponential decay of the complex arose from the glass itself (see below). Consequently, the Ru(bpy)₃²⁺(ads) lifetimes reported

here are those of the slower component obtained by a biexponential, least-squares fit of the data. All fits were over at least 3 lifetimes, and the lifetimes were taken as the time required for the slower component to drop to $1/e$ of the initial ($t = 0$) value.

Results

Adsorption. Ru(bpy)₃²⁺ cation exchanges onto PVG by displacing the slightly acidic silanol protons.²⁴ Silanol groups exist throughout the pore network, but the narrower, tortuous passages connecting the 100 ± 10 Å diameter cavities limit impregnation to the outermost volumes of glass, ca. 10–20% of the total volume.²⁵ Electronic spectra recorded at different locations confirm a uniform distribution of the complex in the impregnated volumes, and the maximum loadings in these experiments, $\leq 1.8 \times 10^{-6}$ mol/g, correspond to surface coverages of $\leq 2\%$ in these volumes.^{24,25}

Spectroscopic Properties. In the 300–600-nm region, the absorption maxima of Ru(bpy)₃²⁺(ads) agree with those found in the aqueous solution spectrum. The absolute extinction coefficient at 452 nm, calculated assuming an optical path length equivalent to the penetration depth and a concentration of moles/unit volume of impregnated glass, is 1.49×10^4 M⁻¹ cm⁻¹, while that calculated from the aqueous solution spectrum is 1.46×10^4 M⁻¹ cm⁻¹. The spin-forbidden MLCT absorptions, which appear in the 460–520-nm region in single crystal spectra,³⁵ are no better resolved on the glass than in aqueous solution, and the relative extinction coefficients in this region differ by $\leq 5\%$ from the corresponding aqueous solution values. Cation exchanging Ru(bpy)₃²⁺ onto the glass, however, increases the half width of the MLCT absorption by 1197 ± 37 cm⁻¹ and decreases the intensity of the 286-nm bipyridine π - π^* transition relative to the aqueous solution spectrum. The ratio of absorbance at 286 nm relative to that at 452 nm is 5.8 ± 0.1 for the adsorbed complex, while that calculated from the aqueous solution spectrum is 6.3 ± 0.1 .

Neither spectrum exhibits a pronounced dependence on temperature. Both in aqueous solution and on the glass, spectra recorded at 5 °C agree in band maxima, half width, and relative extinction coefficient with those recorded at 90 °C. Emission spectra, on the other hand, are temperature dependent. At room temperature, the emission maximum of the adsorbed complex occurs at 605 ± 3 nm, whereas in aqueous solution the maximum occurs at 615 ± 3 nm. Increasing the temperature to 85 °C shifts both maxima to the red: ca. 4 nm in aqueous solution and 7 nm for the adsorbed complex. Emission intensity declines and the band broadens, but at all temperatures, the band shapes are equivalent in both media.

Bipyridine vibrations resonant with the 452-nm MLCT transition of Ru(bpy)₃²⁺(ads) differ by ≤ 1 cm⁻¹ from the corresponding aqueous solution values, and in both media, the frequencies are independent of temperature from 5 to 90 °C.^{10,27} Adsorption onto the glass, however, reduces the intensity of the prominent 1492-cm⁻¹ vibration. At room temperature, the relative intensity of the 1492-cm⁻¹ vibration of Ru(bpy)₃²⁺(ads) is 75% of the corresponding aqueous solution value.¹⁰ In the absence of a standard applicable to both the glass and solution, quantitating the intensities of the resonance Raman bands as a function of temperature is difficult since, to some extent, all band intensities vary with temperature in both media. These changes are random, however, and within experimental error, the relative intensity of the 1492-cm⁻¹ vibration of the adsorbed complex remains 25% less than the corresponding aqueous solution value in spectra recorded at 85 °C.

Excited-State Dynamics. At each temperature, the decay of the *Ru(bpy)₃²⁺ in degassed aqueous solution is described by a single exponential. Values of Φ_{em} and τ measured in degassed aqueous solution (Table 1) are in excellent agreement with the

(29) Calvert, J. G.; Pitts, J. N. *Photochemistry*; John Wiley: New York, 1966; p 780.

(30) Wong, P. K.; Allen, A. O. *J. Phys. Chem.* 1970, 74, 774.

(31) Demas, J. N.; Crosby, G. A. *J. Phys. Chem.* 1971, 75, 991.

(32) (a) Morgan, J. *Introduction to Geometrical and Physical Optics*; McGraw-Hill: New York, 1953; pp 223–227. (b) Robertson, J. K. *Introduction to Optics, Geometrical and Physical*, 4th ed.; Van Nostrand: New York, 1954; pp 178–182.

(33) Shi, W. Ph.D. Thesis, City University of New York, 1986.

(34) Serpone, N.; Hoffman, M. Z. *J. Phys. Chem.* 1987, 91, 1737.

(35) Felix, F.; Ferguson, J.; Gudel, H. U.; Ludi, A. *J. Am. Chem. Soc.* 1980, 102, 4096.

Table 1. Measured and Calculated (in Parentheses) Values of τ and Φ_{em} of $\text{Ru}(\text{bpy})_3^{2+}$ in Aqueous Solution and Adsorbed onto PVG vs Temperature

<i>T</i> , °C	H ₂ O		PVG	
	τ_m , ns	Φ_{em}	τ_m , ns	Φ_{em}
5	720 ± 25 (721)	0.052 ± 0.003 (0.051)	1049 ^a 1061 ^b 1034 ^c 1052 ^d 1049 ± 15 (1044)	0.082 ^a 0.073 ^b 0.075 ^c 0.081 ^d 0.078 ± 0.004 (0.077)
15	690 ± 21 (677)	0.048 ± 0.003 (0.048)	887 ^a 883 ^b 907 ^c 892 ± 15 (891)	0.066 ^a 0.059 ^b 0.060 ^c 0.067 ^d 0.063 ± 0.004 (0.064)
25	600 ± 20 (616)	0.042 ± 0.002 (0.043)	747 ^a 748 ^b 750 ^c 770 ^d 754 ± 16 (776)	0.052 ^a 0.047 ^b 0.049 ^c 0.053 ^d 0.050 ± 0.002 (0.052)
35	527 ± 15 (529)	0.035 ± 0.002 (0.037)	650 ^a 688 ^b 699 ^c 699 ^c 682 ^d 680 ± 30 (674)	0.043 ^a 0.037 ^b 0.037 ^b 0.041 ^c 0.041 ^d 0.041 ± 0.002 (0.041)
45	420 ± 18 (422)	0.029 ± 0.002 (0.030)	590 ^a 592 ^b 597 ^c 585 ^d 591 ± 6 (585)	0.034 ^a 0.030 ^b 0.031 ^c 0.032 ^d 0.032 ± 0.001 (0.032)
55	350 ± 25 (328)	0.023 ± 0.002 (0.023)	520 ^a 511 ^b 519 ^c 521 ^d 518 ± 7 (519)	0.028 ^a 0.024 ^b 0.025 ^c 0.025 ^d 0.026 ± 0.002 (0.025)
65	244 ± 10 (241)	0.017 ± 0.001 (0.017)	466 ^a 459 ^b 462 ^c 484 ^d 468 ± 16 (461)	0.022 ^a 0.020 ^b 0.021 ^c 0.020 ^d 0.021 ± 0.001 (0.021)
75	157 ± 10 (168)	0.012 ± 0.001 (0.012)	408 ^a 404 ^b 443 ^c 392 ^d 412 ± 20 (408)	0.018 ^a 0.017 ^b 0.018 ^c 0.017 ^d 0.018 ± 0.001 (0.018)
85	123 ± 8 (118)	0.0091 ± 0.001 (0.0083)	340 ^a 347 ^b 360 ^c 338 ^d 346 ± 14 (366)	0.015 ^a 0.014 ^b 0.015 ^c 0.014 ^d 0.015 ± 0.001 (0.016)
77 K			5.8 ± 0.3 ms	

^a 5.08×10^{-7} mol/g. ^b 9.50×10^{-7} mol/g. ^c 1.45×10^{-6} mol/g. ^d 1.75×10^{-6} mol/g.

values reported by Van Houton and Watts¹⁶ (Figure 1), and both sets of data yield a Φ_{em}/τ ratio that is independent of temperature (Figure 2a).

Satisfactory fits of the $^*\text{Ru}(\text{bpy})_3^{2+}(\text{ads})$ emission decay, however, require the biexponential

$$I(t) = A_s \exp(-t/\tau_s) + A_l \exp(-t/\tau_l) \quad (2)$$

A_s and A_l are the weighing factors of the short and long components, and τ_s and τ_l are their respective lifetimes. Analysis of the decays, by means of the Simplex, shows that the longer component dominates, $A_s < A_l$, at temperatures < 15 °C, whereas the short-lived component dominates, $A_s > A_l$, at higher temperatures. However, the lifetime of the fast component, τ_s , is independent of temperature, whereas that of the slower component, τ_l , declines with increasing temperature (Table 2). The different temperature dependencies suggest different origins, and picosecond experiments with impregnated and unimpregnated glasses confirm that the fast component arises from the glass itself. The nature of this short-lived emission is not known. It appears to involve multiphoton excitation since PVG absorbs very little, if at all, at the 355-nm excitation wavelength, and the

fast component is observed only with pulsed laser excitation. Since the fast component arises from the glass itself, the emission lifetimes of $^*\text{Ru}(\text{bpy})_3^{2+}(\text{ads})$ at the different temperatures (Table 1) are those obtained from the slower component, τ_l .

The temperature dependence of Φ_{em} and τ for $\text{Ru}(\text{bpy})_3^{2+}(\text{ads})$ (Figure 3) differs from that in degassed aqueous solution (Figure 1), and the individual values (Table 1) yield a Φ_{em}/τ ratio that declines with increasing temperature (Figure 2b). Since $\Phi_{em}/\tau = \eta_{isc}k_r$, the temperature dependence marks a striking departure from fluid solution behavior. In fluid solution, η_{isc} is temperature independent and assumed to be unity, and by its very nature, k_r is expected to be temperature independent, particularly over a relatively narrow temperature range.

An immediate concern was whether the observed dependence was biased by temperature-dependent self-quenching, impurity quenching, or a redistribution of the adsorbate among the Si-OH and B₂O₃ Lewis acid sites in the glass. Temperature-dependent impurity quenching is discounted since the results were reproducible on seven different samples of the glass and independent of whether the glass was calcined at 650 °C in an oxidizing (air) or reducing (H₂) atmosphere. Self-quenching

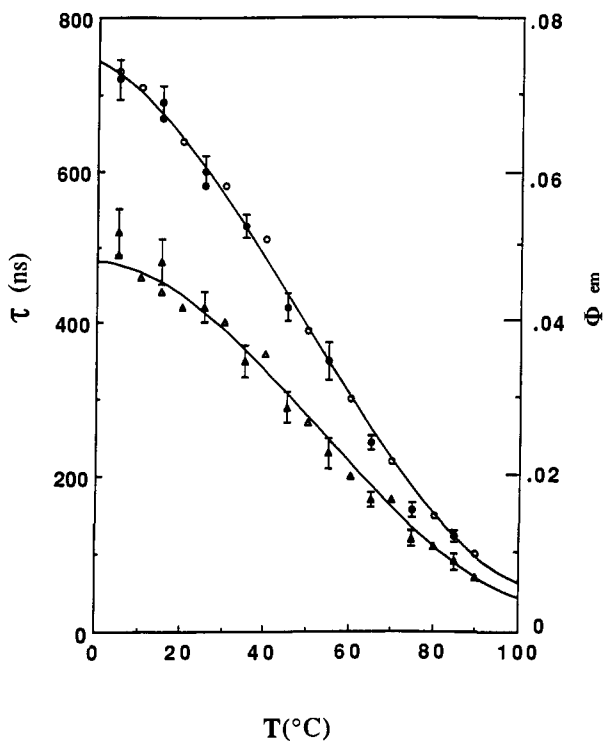


Figure 1. Temperature dependence of Ru(bpy)₃²⁺ emission lifetime (O) and quantum yield (Δ) in degassed aqueous solution. Open points (O, Δ) are from ref 16, while solid points (●, ▲) are values measured in these experiments.

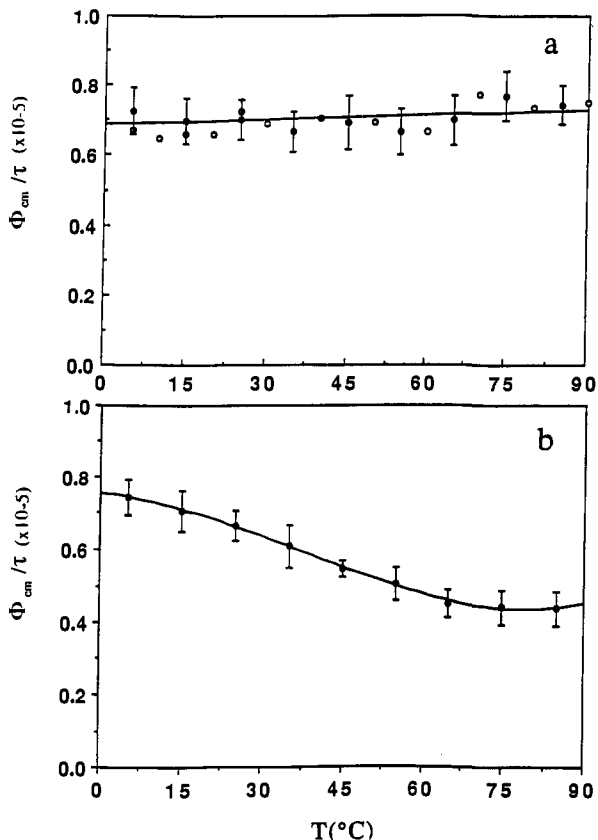


Figure 2. Temperature dependence of the Φ_{em}/τ ratio in (a) aqueous solution and (b) adsorbed onto PVG. The aqueous solution ratios designated by open circles are from ref 16, while the solid circles represent data measured in these experiments.

occurs on PVG, but at room temperature it requires a contact interaction, *i.e.*, loadings $\geq 10^{-4}$ mol/g corresponding to at least monolayer coverage.¹⁰ The maximum loadings in these experi-

Table 2. Temperature Dependence of the Parameters Derived from a Biexponential Fit of the Ru(bpy)₃²⁺(ads) Emission Decays

T, °C	A ₁ ^a	A ₂ ^b	τ_2 , ns	τ_1 , ns
0	0.68	0.32	87 ± 7	1148 ± 16
5	0.61	0.39	79 ± 11	1049 ± 8
15	0.54	0.46	57 ± 12	892 ± 10
25	0.40	0.60	47 ± 3	746 ± 4
35	0.52	0.48	66 ± 6	694 ± 6
45	0.43	0.57	73 ± 15	598 ± 14
55	0.41	0.59	70 ± 5	509 ± 6
65	0.38	0.62	78 ± 8	469 ± 9
75	0.37	0.63	80 ± 6	418 ± 17
85	0.27	0.73	67 ± 11	348 ± 9

^a Relative value = $A_1/A_1 + A_2$. ^b Relative value = $A_2/A_1 + A_2$.

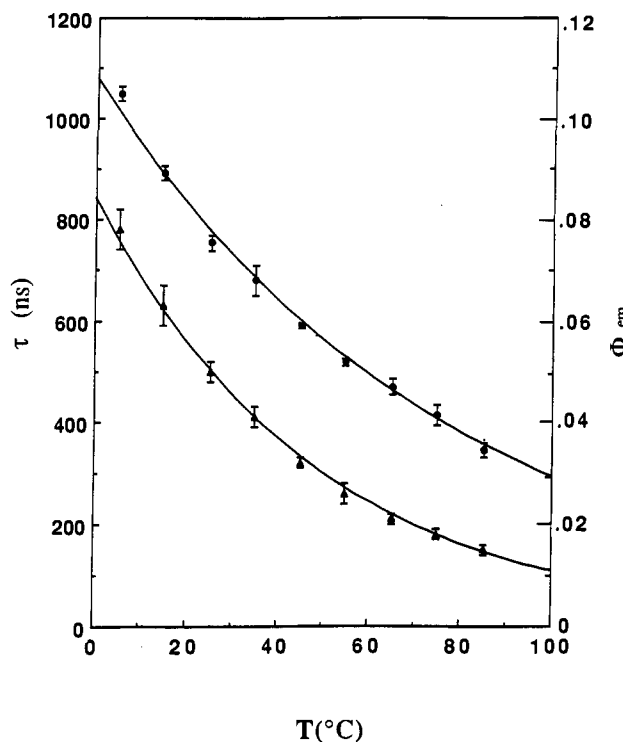


Figure 3. Temperature dependence of the lifetime and quantum yield of Ru(bpy)₃²⁺(ads) calculated from eqs 5 and 9 (solid line) and experimental values of lifetime (O) and quantum yield (Δ).

ments, $\leq 1.8 \times 10^{-6}$ mol/g, correspond to a surface coverage of $\leq 2\%$, with an average spacing of ≥ 55 Å between the adsorbed ions.²⁴ Since this is more than double currently known long range interaction distances,³⁶ self-quenching requires either an exceptionally long range interaction or an increase in adsorbate mobility with increasing temperature. The probability of a long range interaction increases with increasing surface coverage, but the Ru(bpy)₃²⁺(ads) emission quantum yield is independent of loading up to 10^{-4} mol/g.¹⁰ Nor is there evidence of an increase in adsorbate mobility with increasing temperature. Macroscopic diffusion in the glass is extremely slow or nonexistent even at temperatures as high as 1200 °C,³⁷ and in the 273–363 K range, the emission polarization ratio for Ru(bpy)₃²⁺(ads), 0.16 ± 0.02 with 465-nm excitation, is within experimental error of that measured in 77 K hydrocarbon glasses.²⁷ Since rotational motion is expected to accompany translational motion, self-quenching due to an increase in adsorbate mobility is discounted.

Ru(bpy)₃²⁺ cation exchanges onto the glass by displacing the slightly acidic silanol protons.²⁴ A redistribution among these sites and B₂O₃ Lewis acid sites (XPS indicates $2.6 \pm 0.1\%$ B present in the first 50 Å of the glass³⁷) would require some adsorbate mobility and, considering the difference in electron

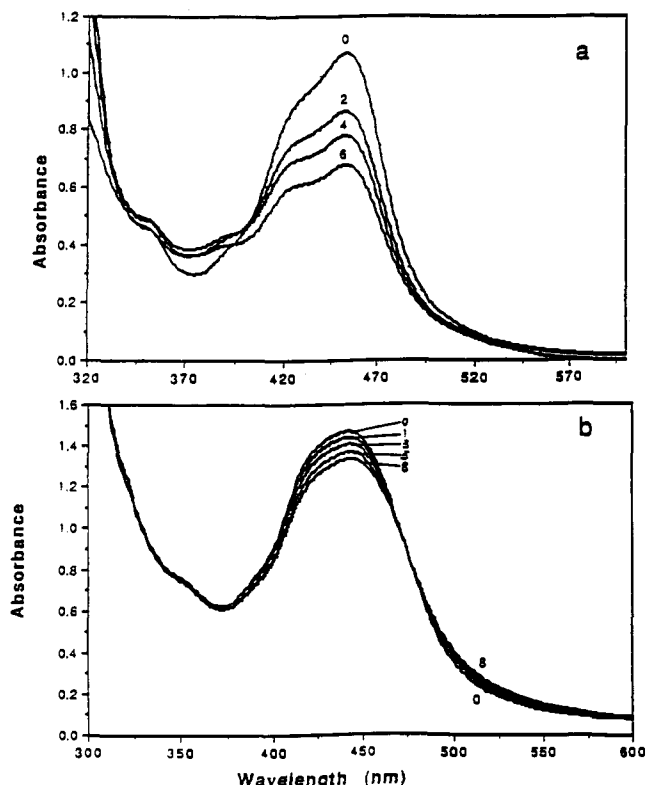


Figure 4. Spectral changes during 350-nm photolyses of $\text{Ru}(\text{bpy})_3^{2+}$ at 83 °C in (a) 0.1 M HCl and (b) adsorbed onto PVG. Numbers refer to photolysis times in hours.

donating and withdrawing properties of the sites, would be expected to occur with some spectral change. As noted adsorbate mobility is severely curtailed, and absorption and resonant Raman spectra of $\text{Ru}(\text{bpy})_3^{2+}(\text{ads})$ are independent of temperature in the 5–90 °C range. In the temperature range examined here, $\text{Ru}(\text{bpy})_3^{2+}$ appears to remain bound to the silanol site onto which it originally adsorbed.

Photochemistry. At 83 °C, a 350-nm photolysis of a degassed 0.1 M HCl solution containing 5.5×10^{-5} M $\text{Ru}(\text{bpy})_3^{2+}$ causes a decline in absorbance at 450 nm, and a corresponding increase at 370 nm (Figure 4a). The spectral changes are similar to those reported by Van Houton and Watts,¹⁶ except that with 350-nm excitation, a shoulder at 500 nm did not appear during the initial stages of photolysis. Nevertheless, the subsequent changes closely resemble those reported by Van Houton and Watts, and indicate bipyridine photolabilization.¹⁶ At 83 °C with 350-nm excitation and 0.1 M HCl, the decrease in absorbance at 452 nm yields a quantum efficiency of bipyridine labilization of $3.8 \pm 0.7 \times 10^{-3}$.

This experiment cannot be duplicated in the glass since, at 83 °C, the concentration of H^+ needed to trap the dissociated ligand is also sufficient to dissolve the glass matrix. Nevertheless, the experiment was repeated since PVG possesses silanol groups that can function as photoproduct scavengers.³⁸ However, spectra recorded during 350-nm photolysis of a PVG sample containing 1.2×10^{-6} mol of $\text{Ru}(\text{bpy})_3^{2+}(\text{ads})$ at 83 °C (Figure 4b) are inconsistent with ligand labilization. The decline in absorbance at 452 nm accompanied by an increase in the 510–520-nm region in the ratio of $2.2 \pm 0.1:1$ is similar to the spectral changes observed during the photoinduced disproportionation of $\text{Ru}(\text{bpy})_3^{2+}(\text{ads})$.²⁴ The quantum efficiency of $\text{Ru}(\text{bpy})_3^{2+}(\text{ads})$ disappearance, $4.1 \pm 0.5 \times 10^{-4}$, is also within the range of values found for the disproportionation reaction.²⁴

Table 3. Parameters Derived from the Temperature Dependence of τ and Φ_{em} of $\text{Ru}(\text{bpy})_3^{2+}$ in Aqueous Solution

	lit. values ^a	calcd ^b
ΔE , cm^{-1}	3559	3583 ± 76
k_r , s^{-1}	6.96×10^4	$7.0 \pm 0.1 \times 10^4$
k_{nr} , s^{-1}	1.222×10^6	1.2×10^6
k_1 , s^{-1}	10^{13}	10^{13}

^a Reference 16. ^b Calculated from data gathered in our experiments.

Discussion

$\text{Ru}(\text{bpy})_3^{2+}$ cation exchanges onto PVG without disruption of its primary coordination sphere, and at each temperature it retains the spectroscopic properties found in aqueous solution.^{10,11,24,28} Bipyridine vibrations resonant with the 452-nm MLCT absorption also differ by ≤ 1 cm^{-1} from the corresponding aqueous solution values.¹⁰ Nevertheless, the 1197 ± 37 cm^{-1} increase in the half width of the MLCT absorption and the declines in the relative intensities of the 286-nm bipyridine localized $\pi-\pi^*$ transition and 1492- cm^{-1} vibration imply that adsorption induces some molecular distortion. The change in the relative extinction coefficient, although smaller, is in the same direction as found when $\text{Ru}(\text{bpy})_3^{2+}$ intercalates into hectorite, where it is attributed to a distortion of the bipyridine ligand.³⁹ The probability of light absorption, however, is proportional to the Franck–Condon factors coupling the states. Consequently, differences from fluid solution structures in either the ground state and/or excited state can lead to changes in absorptivity. In PVG, the data point to structural differences principally in the excited state.

Resonant Raman frequencies are a ground-state property, whereas the band intensities are related to the nuclear displacements that distort the ground-state configuration to that of the excited-state.⁴⁰ In the 5–85 °C range, the frequencies of the bipyridine vibrations resonant with 452-nm MLCT transition are equivalent in both media. With the exception of two additional vibrations at 1044 and 1266 cm^{-1} , RR spectra recorded with 364-nm excitation show that the same seven bipyridine vibrations resonant with the MLCT transition are also resonant with the near-UV $\pi-\pi^*$ transitions.⁴¹ The absence of a change in frequency indicates equivalent ground-state structures in both media, whereas the reduced intensity of the prominent 1492- cm^{-1} band points to a change in excited-state geometry. Consequently, the decrease in absorptivity of the bipyridine localized $\pi-\pi^*$ transition and the 1197 ± 37 cm^{-1} increase in the half width of the MLCT transition are attributed to “matrix effects”, in which the rigidity of the glass curtails the bipyridine distortions that accompany optical excitation. As a result, the ¹MLCT state and bipyridine localized π^* state of $\text{Ru}(\text{bpy})_3^{2+}(\text{ads})$ differ structurally from those in aqueous solution.

In degassed aqueous solution, the temperature dependence of the emission lifetime, $\tau(T)$, and quantum yield, $\Phi_{\text{em}}(T)$, of $\text{Ru}(\text{bpy})_3^{2+}$ are given by¹⁶

$$\tau(T) = [(k_{1r} + k_{1q}) + k_{2q} \exp(-\Delta E/kT)]^{-1} \quad (3)$$

$$\Phi_{\text{em}}(T) = k_{1r}\tau(T) \quad (4)$$

Using the Van Houton–Watts notation, k_{1r} and k_{1q} are the rate constants for radiative and nonradiative decay of the emissive MLCT state, while ΔE and k_{2q} represent the activation barrier encountered in populating the LF manifold and the rate constant for nonradiative decay from this manifold. Fitting the aqueous solution data gathered in our experiments (Table 1) with eqs 3 and 4 yields values of the different parameters (Table 3) that are

(39) Krenske, D.; Abdo, S.; Van Damme, H.; Cruz, M.; Fripiat, J. J. *J. Phys. Chem.* **1980**, *84*, 2447; **1981**, *85*, 797.

(40) Washel, A. *Annu. Rev. Biophys. Bioeng.* **1977**, *6*, 273.

(41) Bradley, P. G.; Kress, N.; Hornberg, B. A.; Dallinger, R. F.; Woodruff, W. H. *J. Am. Chem. Soc.* **1981**, *103*, 7441.

(37) Mendoza, E. A.; Wolkow, E.; Sunil, D.; Wong, P.; Sokolov, J.; Rafailovich, M. H.; den Boer, M.; Gafney, H. D. *Langmuir* **1991**, *7*, 3046.

(38) Gafney, H. D. In *Photochemistry on Solid Surfaces*; Anpo, M., Matsuura, T., Eds.; Elsevier: Amsterdam, 1989; p 272.

in excellent agreement with the values reported by Van Houton and Watts.¹⁶ Aqueous solution measurements were carried out to establish the reliability of our procedures, and to obtain, under as similar a set of conditions as possible, a reference to which the glass data could be compared.

PVG is a spinodally decomposed, borosilicate glass in which the borate phase is acid leached leaving a random three-dimensional array of interconnected pores.^{37,42-45} Since the average spacing between the adsorbed ions in these experiments, ≥ 55 Å, exceeds known interaction distances,³⁶ the absence of adsorbate mobility precludes temperature-dependent self-quenching. The values of Φ_{em} and τ for Ru(bpy)₃²⁺(ads) (Table 1) are also independent of initial loading, calcination conditions, and degassing procedures. Consequently, temperature-dependent quenching by trace amounts of O₂, some undefined impurity, or a redistribution among different sites is also discounted. Ru(bpy)₃²⁺(ads) exists as a dispersed, immobilized molecular entity, and the temperature dependence of Φ_{em} and τ reflects the temperature dependence of its excited-state dynamics.

Regardless of loading, Ru(bpy)₃²⁺(ads) lifetime *vs* temperature data fit (Figure 3) the abbreviated form of eq 3

$$\tau(T) = [k_0 + k_1 \exp(-\Delta E/kT)]^{-1} \quad (5)$$

where $k_0 = k_{1r} + k_{1q}$, $k_1 = k_{2q}$, and ΔE represents the activation energy. The data gathered here yield $3.30 \pm 0.6 \times 10^5$ s⁻¹, $3.18 \pm 0.5 \times 10^8$ s⁻¹, and 1168 ± 160 cm⁻¹ for the respective parameters. In a cellulose acetate matrix and over a wider temperature range, Ru(bpy)₃²⁺ lifetime *vs* temperature data require a three-term equation¹⁸

$$\tau(T) = [k_0 + k_1 \exp(-\Delta E_1/kT) + k_2 \exp(-\Delta E_2/kT)]^{-1} \quad (6)$$

where k_2 and ΔE_2 correspond to an additional decay pathway. A three-term equation will obviously fit the data equally well. Nevertheless, eq 6 was tested, and it was immediately apparent that the two models were identical since ΔE_1 from eq 6 (51 ± 14 cm⁻¹) is $\leq kT$ in the 5–90 °C range. Both equations yield equivalent activation barriers, 1168 ± 160 (eq 5) and 1136 ± 67 cm⁻¹ (eq 6), although for simplicity the value 1168 ± 160 cm⁻¹ will be used.

A recent review of lifetime *vs* temperature data for a number of Ru(II) and Os(II) diimines in fluid solution reports that, when the activation energy is 300–800 cm⁻¹ and k_1 is 10^6 – 10^8 s⁻¹, a low-lying, nonemissive MLCT state, rather than a d–d state, participates in the relaxation process.²² When Ru(bpy)₃²⁺ is incorporated into a cellulose acetate matrix, $k_1 = 1.73 \times 10^6$ s⁻¹, and the barrier reduces from *ca.* 3500 cm⁻¹ in aqueous solution to 810 ± 120 cm⁻¹ in the matrix.¹⁸ The reduction is attributed to “matrix effects”, where the rigidity of the matrix curtails the metal–ligand distortions accompanying the $(d\pi)^5(\pi^*)^1-(d\pi)^5-(d\sigma^*)^1$ transition.²² As a result, nonradiative decay in the more rigid medium occurs through a lower energy MLCT state rather than through the higher energy LF manifold. RR spectra recorded in our experiments do not probe the metal–ligand vibration *per se*, but the increased half width of the MLCT transition and the reduced intensities of the 1492-cm⁻¹ vibration and 286-nm π – π^* absorption attest to matrix effects in this glass. In addition, the observed photochemistry—photoinduced disproportionation rather than photolabilization—supports the population of a nonemissive charge transfer state rather than a dd state.^{22,24,45,46} Like other

more rigid media,¹⁸ PVG apparently induces a matrix effect that promotes the population of a nonemissive MLCT state, which in Ru(bpy)₃²⁺(ads) lies 1168 ± 160 cm⁻¹ above the emissive manifold.

Although eq 5 reproduces the temperature dependence of the Ru(bpy)₃²⁺(ads) lifetime, when substituted into eq 4, it fails to reproduce the observed temperature dependence of Φ_{em} . Alternatively, if $\tau(T)$ and $\Phi_{em}(T)$ data are fit independently with eqs 5 and 4, different values for the activation energy and the rate constants are obtained. Since $\Phi_{em}/\tau = \eta_{isc}k_r$, eq 4 assumes that $\eta_{isc}k_r$ is independent of temperature and η_{isc} is unity. Van Houton and Watts' data,¹⁶ as well as our own, show that Φ_{em}/τ is indeed independent of temperature in aqueous solution (Figure 2). However, Φ_{em}/τ for Ru(bpy)₃²⁺(ads) declines by 42% in the 5–85 °C range (Figure 2). Adsorption onto this glass leads to a fundamental change in the decay dynamics prior to emission that is not obvious from the spectroscopic or lifetime data.

Our data do not distinguish whether η_{isc} and/or k_r are temperature dependent. In our opinion, however, attributing the temperature dependence of Φ_{em}/τ to k_r is inconsistent with the very nature of a spontaneous emission process. Interposing an activation barrier in a spontaneous emission process is arbitrary, specifically in this case, where the activation energy would have to be negative to account for the observed dependence. Furthermore, spectroscopic data offer no indication that the intrinsic parameters that govern k_r change with temperature. According to Einstein's law for spontaneous emission, $k_r \propto E_{em}^3$ where E_{em} is the emission energy.⁴⁷ Both in aqueous solution and on the glass, as the temperature increases from 5 to 90 °C, the emission maxima shift ≤ 7 nm to the red. However, these shifts, or assuming similar shifts in the 0–0 emission energies, correspond to declines of $\leq 5\%$ in k_r , which is insufficient to account for the observed 42% decline in the Φ_{em}/τ ratio for Ru(bpy)₃²⁺(ads). Demas and Crosby have expressed the radiative rate constant¹²

$$k_r = \epsilon(S)K[M_{so}]^2(E_T/E_S)/(E_T - E_S)^2 \quad (7)$$

in terms of the molar extinction coefficient for absorption to the ¹MLCT state, $\epsilon(S)$, a constant K , the spin–orbit coupling constant, M_{so} , and the singlet- and triplet-state energies. The latter implies that the temperature dependence of k_r would be evident in the complex's spectroscopic parameters. In both aqueous solution and on the glass, however, absorption spectra recorded at 5 °C agree in band maxima, half width, and relative extinction coefficients with those recorded at 90 °C. Since the spectroscopic data offer no indication that k_r is temperature dependent, we attribute the observed temperature dependence of Φ_{em}/τ in this glass to the intersystem crossing efficiency, η_{isc} .

A decline in η_{isc} with increasing temperature could be due to either thermally activated nonradiative decay of the ¹MLCT state competitive with intersystems crossing or intersystem crossing specifically to a nonemissive state. The latter might involve, for example, population of the nonemissive MLCT state²² that lies 1168 ± 160 cm⁻¹ above the emissive state, followed by nonradiative decay to the ground state. We discount the latter mechanism, however, since lifetime data indicate that the emissive and nonemissive MLCT states (right side of Figure 5) thermally equilibrate. If intersystem crossing to a specific state is followed by thermal equilibration among the emissive and nonemissive levels, then regardless of the state initially populated, the temperature dependence of Φ_{em} would parallel the temperature dependence of τ , which is not the case. Rather, we propose that η_{isc} declines due to the thermally activated population of a higher energy state. Increasing the temperature increases the population of this state which lies ΔE_2 above the ¹MLCT (left side of Figure 5), and from this level, nonradiative decay occurs competitive with intersystem crossing to the emissive manifold. Assuming that the higher energy state and ¹MLCT level thermally

(42) Elmer, T. H.; Fehlner, A.; Nordberg, M. E. *J. Am. Ceram. Soc.* **1970**, *53*, 171.

(43) Elmer, T. H.; Chapman, I. D.; Nordberg, M. E. *J. Phys. Chem.* **1962**, *66*, 1517.

(44) Iler, R. K. *The Chemistry of Silica*; Wiley-Interscience: New York, 1979; p 551.

(45) Snyder, L. R.; Ward, J. W. *J. Phys. Chem.* **1966**, *70*, 3941.

(46) Meisel, D.; Matheson, M. S.; Mulac, W. A.; Rabini, J. *J. Phys. Chem.* **1977**, *81*, 1449.

(47) Yersin, H.; Gallhuber, E. *J. Am. Chem. Soc.* **1984**, *106*, 6582.

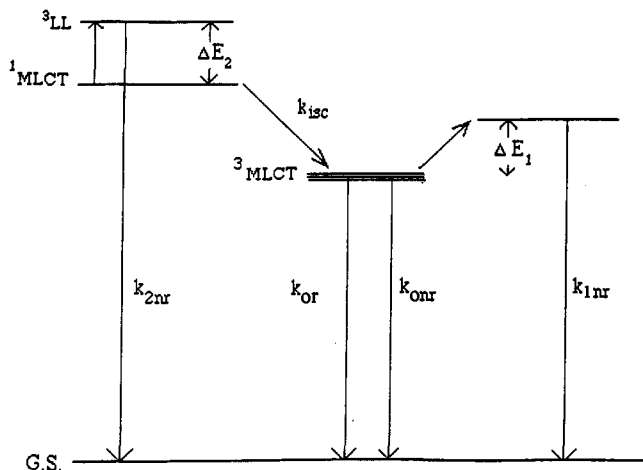


Figure 5. Energy level diagram for Ru(bpy)₃²⁺(ads).

equilibrate, η_{isc} is given by

$$\eta_{isc} = k_{isc} / (k_{isc} + k_{2nr} \exp(-\Delta E_2/kT)) \quad (8)$$

where ΔE_2 is the energy gap, and k_{isc} and k_{2nr} are the rate constants for intersystem crossing to the emissive manifold and nonradiative decay from the higher energy level. Substituting eqs 5 and 8 into the expression $\Phi_{em} = \eta_{isc} k_r \tau$ yields

$$\Phi_{em} = [k_{isc} / \{k_{isc} + k_{2nr} \exp(-\Delta E_2/kT)\}] [k_r / \{k_{or} + k_{onr} + k_{1nr} \exp(-\Delta E_1/kT)\}] \quad (9)$$

Although values of k_{or} , k_{onr} , k_{1nr} , and ΔE_1 are available from the lifetime data, the parameters were treated as unknowns to test the consistency of the lifetime and quantum yield models. Fitting eq 9 to the observed temperature dependence of Φ_{em} by means of the Simplex yields $k_{or} = 1.1 \pm 0.1 \times 10^5 \text{ s}^{-1}$, $k_{2nr}/k_{isc} = 101 \pm 17$, $\Delta E_2 = 1117 \pm 70 \text{ cm}^{-1}$, $k_{or} + k_{onr} = 2.56 \pm 0.5 \times 10^5 \text{ s}^{-1}$, $k_{1nr} = 2.36 \pm 0.8 \times 10^5 \text{ s}^{-1}$, and $\Delta E_1 = 1122 \pm 100 \text{ cm}^{-1}$. The calculated values of $k_{or} + k_{onr}$, k_{1nr} , and ΔE_1 are in excellent agreement with those calculated from the lifetime data, *i.e.*, $k_{or} + k_{onr} = 3.30 \pm 0.6 \times 10^5 \text{ s}^{-1}$, $k_{1nr} = 3.18 \pm 0.5 \times 10^8 \text{ s}^{-1}$, and $\Delta E_1 = 1168 \pm 160 \text{ cm}^{-1}$, and establish a self-consistency between the two independent sets of measurements. Also, consistent with the spectroscopic similarities, which suggest that k_{or} should be similar in the two media, the value of k_{or} obtained from the above analysis is in excellent agreement with the aqueous solution value when corrected for the differences in the refractive indices of the media. The radiative rate constant is given by⁴⁸

$$k_r = 2900 n^2 \nu_o^2 \int \epsilon d\nu \quad (10)$$

where n , ϵ , and ν_o are the refractive index of the medium, the molar extinction coefficient, and the absorption band maximum, respectively. Assuming the parameters can be approximated by spin-allowed MLCT, with the exception of the refractive indices, the values of the parameters are essentially identical in PVG and water. Taking 1.31 as the refractive index of water and 1.51 as that of PVG and correcting the value of k_{or} measured in aqueous solution, $0.70 \pm 0.10 \times 10^5 \text{ s}^{-1}$, for the difference in refractive index yields $0.93 \pm 0.13 \times 10^5 \text{ s}^{-1}$ for k_{or} in the glass, which is within experimental error of the value obtained from the above analysis, $1.1 \pm 0.1 \times 10^5 \text{ s}^{-1}$.

The lifetime and photochemical data for Ru(bpy)₃²⁺(ads) point to a low-energy nonemissive MLCT state, rather than a dd manifold, in thermal equilibrium with the emissive MLCT state. However, the model consistent with both $\Phi_{em}(T)$ and $\tau(T)$ requires

(48) Parker, C. A. *Photoluminescence of Solutions*; Elsevier: Amsterdam, 1968; p 23.

a second energy level that lies $1117 \pm 70 \text{ cm}^{-1}$ above the ¹MLCT state. This energy gap is within the range of a molecular vibration, and spectroscopic data show that adsorption increases the half width of the MLCT transition and reduces the intensities of the bipyridine localized 286-nm $\pi-\pi^*$ transition and the 1492-cm⁻¹ bipyridine vibration resonant with the MLCT absorption. Activation of a specific molecular vibration could achieve a "critical geometry",⁴⁹ although in this case the geometry achieved thermally promotes relaxation to the ground state competitive with intersystem crossing to the emissive manifold, *i.e.*, η_{isc} declines with increasing temperature. Instead, we assign this higher energy level to an electronic state since thermal population of a specific electronic state, as opposed to the activation of a molecular vibration, appears to be more consistent with data that show that, under certain conditions, η_{isc} of Ru(II) diimines can either increase or decrease with increasing temperature.

Adding ΔE_2 to the energy of the 452-nm MLCT transition places this higher energy state $23240 \pm 100 \text{ cm}^{-1}$ above the ground state. Polarized absorption spectra of Ru(bpy)₃²⁺ in [Zn(bpy)₃-Br₂]-6H₂O crystals reveal a number of σ and π polarized absorptions in the 25000–28000-cm⁻¹ region.³⁵ Ferguson and co-workers assign the transitions exhibiting a strong π polarization to the lowest triplet state bpy in the Ru(II) complex. Although the energies corresponding to the absorption maxima are somewhat larger than the calculated $23240 \pm 100 \text{ cm}^{-1}$ energy, the 0–0 transition energies will be lower. Based on the estimated width of the 286-nm bipyridine localized $\pi-\pi^*$ transition, 0–0 transition energies could lie as much as 4000 cm⁻¹ below the absorption maxima.⁵⁰ We propose that the thermally accessible higher energy state lying $1117 \pm 70 \text{ cm}^{-1}$ above the ¹MLCT state is a ligand localized triplet state, ³LL. Assuming that the majority of molecules are in the ³LL state at the higher temperatures, the ³LL state undergoes nonradiative decay to the ground state, whereas the ¹MLCT state undergoes intersystem crossing with an efficiency equivalent to that in fluid solution, *i.e.*, unity. Neither process is temperature dependent. Rather, the temperature dependence arises from a thermal equilibration between the ¹MLCT and ³LL states, and as a result, the apparent value of η_{isc} for Ru(bpy)₃²⁺(ads) declines with increasing temperature. In this case, the glass does not appear to reduce the intersystem crossing efficiency, *per se*. Rather, it promotes, perhaps by curtailing specific ligand vibrations, the population of a ³LL state. Most likely, this is a matrix effect, but the results obtained in this glass may be symptomatic of a more general phenomenon in Ru(II) diimines.

The Φ_{em}/τ ratio for Ru(bpy)₃²⁺ in aqueous solution is independent of temperature, but in other cases where both emission lifetime and quantum yield data are available, the published data yield ratios that are temperature dependent. The emission lifetimes and quantum yields of Ru(bpy)₂(diaz)²⁺ (diaz = 4,5-diazafuorene), for example, indicate that the Φ_{em}/τ ratio approximately doubles as temperature rises from *ca.* 200 to 236 K.⁵¹ Schmehl and Cherry and their co-workers suggest that k_r changes with temperature, but in the absence of a spectroscopic change,⁵² the temperature dependence may reflect a change in η_{isc} . Nakamura reports that the intersystem crossing efficiency of Ru(bpy)₂(dmby)²⁺ (dmby = 3,3'-dimethyl-2,2'-bipyridine) at 77 K is *ca.* 10² times larger than that at 298 K.⁵³ In two other complexes, Ru(bpy)₂(py)₂²⁺ and Ru(bpy)₂NPP²⁺ (NPP = 4-nitro-2-(2-pyridyl)phenyl), the activation barriers obtained from the reported emission quantum yields differ from those obtained from

(49) Turro, N. J. *Modern Molecular Photochemistry*; Benjamin/Cummings: Menlo Park, CA, 1978; p 170.

(50) The 0–0 energy was calculated assuming a Gaussian band shape for the 286-nm $\pi-\pi^*$ transition, and assuming that 0–0 transition energy occurs at the point where the absorption is 5% of the maximum.

(51) Wacholtz, W. M.; Auerbach, R. A.; Schmehl, R. H.; Ollino, M.; Cherry, W. R. *Inorg. Chem.* **1985**, *24*, 1758.

(52) Schmehl, R. H., private communication, 1991.

(53) Nakamaru, K. *Bull. Chem. Soc. Jpn.* **1982**, *55*, 2697.

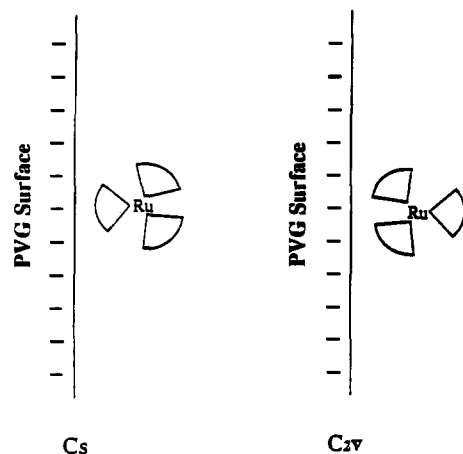


Figure 6. Idealized geometries of $\text{Ru}(\text{bpy})_3^{2+}$ adsorbed onto the surface of the glass.

the lifetime data.⁵⁴ Since $\tau(T)$ reflects thermal equilibration within the lower energy MLCT states, whereas $\Phi_{\text{em}}(T)$ reflects the latter and the apparent intersystem crossing efficiency, differences in the activation energies may also indicate temperature-dependent events prior to or concurrent with the population of the emissive manifold.

Currently available data show that in these mixed-ligand complexes, the intersystem crossing efficiency can either increase or decrease with temperature. Cation exchanging $\text{Ru}(\text{bpy})_3^{2+}$ onto PVG reduces the complex's symmetry from D_3 to C_{2v} or C_s , depending on the orientation on the glass surface (Figure 6). These are idealized geometries, but adsorption onto the anionic surface of this glass, which exhibits a ζ potential of -27 mV in water,⁵⁵ differentiates the initially equivalent bpy ligands. Of course, it can be reasonably argued that the perturbation is small since the electronic spectra of the complex in the two media are similar. On the other hand, there is a reduction in the relative intensity of the 286-nm absorption, and in the 5–90 °C range, the emission polarization ratio of $\text{Ru}(\text{bpy})_3^{2+}(\text{ads})$ is equivalent to that in 77 K hydrocarbon glasses.^{10,33} In our opinion, the latter in particular argues for a relatively strong interaction, although it may not be equivalent in magnitude to that found in a mixed-ligand complex. Nevertheless, in $\text{Ru}(\text{II})$ diimines, nonradiative decay to the $^3\text{MLCT}$ manifold is an energy dissipative process that involves charge delocalization among all ligands since, with few exceptions, emission occurs from the lowest energy

(54) Revecó, P.; Schmehl, R. H.; Cherry, W. R.; Fronczek, F. R.; Selbin, J. *Inorg. Chem.* **1985**, *24*, 4078.

(55) Basu, A.; Gafney, H. D.; Perette, D. J.; Clark, J. B. *J. Phys. Chem.* **1983**, *87*, 4532.

$^3\text{MLCT}$ state corresponding to a specific metal–ligand pair regardless of the state populated on adsorption. In this sense, intersystem crossing will depend on the surrounding ligands, and the above data suggest that an asymmetric environment, whether it arises from different ligands or, as in the case of $\text{Ru}(\text{bpy})_3^{2+}(\text{ads})$, a differentiation due to adsorption, creates a situation in which the apparent intersystem crossing efficiency is temperature dependent. We propose that the temperature dependence arises from the population of an ^3LL state which opens a nonradiative decay pathway. In which case, whether the apparent η_{isc} increases with increasing temperature, as appears to be the case in $\text{Ru}(\text{bpy})_2(\text{diaz})^{2+}$,⁵¹ or decreases with increasing temperature, as with $\text{Ru}(\text{bpy})_3^{2+}(\text{ads})$ and $\text{Ru}(\text{bpy})_2(\text{dmby})^{2+}$,⁵³ will depend on the relative energies and populations of the $^1\text{MLCT}$ and ^3LL states. Experiments to test these ideas are in progress, but clearly intersystem crossing efficiencies are not necessarily temperature independent, and in mixed-ligand complexes and more rigid media much closer experimental scrutiny is deserved.

Conclusion

$\text{Ru}(\text{bpy})_3^{2+}$ cation exchanged onto porous Vycor glass retains the spectroscopic properties found in aqueous solution. As found in other more rigid media, the temperature dependence of the lifetime and photochemical behavior of the adsorbed complex point to a thermal equilibration among the emissive MLCT state and a nonemissive MLCT state that lies 1168 ± 160 cm^{-1} above the emissive state. Also, unlike aqueous solution, where the Φ_{em}/τ ratio is independent of temperature, that for the adsorbed complex declines by 42% in the 5–90 °C range. A model consistent with both $\Phi_{\text{em}}(T)$ and $\tau(T)$ data suggests that the temperature dependence arises from a thermal equilibration among the $^1\text{MLCT}$ state and a ^3LL state lying 1117 ± 70 cm^{-1} above the $^1\text{MLCT}$ state. Intersystem crossing from the $^1\text{MLCT}$ state occurs with an efficiency equivalent to that in aqueous solution, but population of the ^3LL state leads to competitive nonradiative decay. Comparison with published data suggests that asymmetric coordination arising either from different ligands or with $\text{Ru}(\text{bpy})_3^{2+}(\text{ads})$ differentiation of the ligands by adsorption onto the anionic surface of the glass leads to a temperature-dependent intersystem crossing efficiency. In these cases, intersystem crossing either increases or decreases with temperature depending on the relative energies of the $^1\text{MLCT}$ and ^3LL states.

Acknowledgment. Support of this research by the Research Foundation of the City University of New York and the National Science Foundation (CHE-8913496) is gratefully acknowledged. N.S. gratefully acknowledges support from NSERC (Ottawa). H.D.G. thanks Dr. David L. Morse of Corning Inc. for the samples of porous Vycor glass and Dr. Johna Leddy for a very helpful discussion.